Freezing of adhesive hard spheres

Carlos F. Tejero
Facultad de Ciencias Físicas, Universidad Complutense de Madrid, E-28040 Madrid, Spain

Marc Baus
Faculté des Sciences, Université Libre de Bruxelles, Code Postale 231, B-1050 Brussels, Belgium
(Received 19 July 1993)

A theoretical study of the freezing of adhesive hard spheres within the generalized-effective-liquid approximation has been performed. The liquid-solid phase diagram exhibits most of the trends observed for simple liquids. There is, however, no triple point because the solid phase becomes mechanically unstable in the region where the liquid-solid transition crosses the percolation transition. A useful closed-form expression for the free energy of the fluid phases is also given.

PACS number(s): 64.70.Dv, 64.10.+h

I. INTRODUCTION

In recent years much of the successful work on the fluid-solid transition [1] has been restricted to the freezing of hard spheres (HS) for which the nonperturbative density-functional theories [2] provide very accurate results for the fluid-solid coexistence data. The HS system lacks, however, one of the most important features of the real freezing transition, since its phase diagram exhibits no temperature dependence. The straightforward extension of the above theories of freezing to more realistic potentials has encountered difficulties and, at present, most of the current work is therefore concerned with setting up perturbation schemes for smooth potentials that use the HS solid as a reference system [3], in analogy with the perturbation theories for the liquid phase [4]. In the present study we consider the freezing of adhesive hard spheres (AHS), a system situated at the borderline between the above domains, since its potential is still singular but its phase diagram is temperature dependent and in many respects similar to that of more realistic systems.

The physics of AHS is most easily understood by starting from a system of particles interacting with the following "square well" (SW) pair potential $V(r)$:

$$V(r) = \begin{cases} \infty & (0 < r/\sigma < 1) \\ -V_0 & (1 < r/\sigma < 1+\epsilon) \\ 0 & (1+\epsilon < r/\sigma)\ , \end{cases} \tag{1.1}$$

consisting of a HS part (σ being the HS diameter) and an attractive ($V_0 > 0$) square well of width $\epsilon\sigma$ and depth V_0. As shown by Baxter [5], the equations underlying the Percus-Yevick (PY) approximation [4] can be solved in closed form for a fluid phase interacting with the SW potential of Eq. (1.1) if one takes, moreover, the limit of zero width ($\epsilon \to 0$) and infinite depth ($V_0 \to \infty$) in such a way as to keep constant the contribution of the attractive square well part of (1.1) to the second virial coefficient B_2 [4], viz.,

$$\frac{B_2^{\mathrm{HS}} - B_2^{\mathrm{SW}}}{B_2^{\mathrm{HS}}} \equiv [\exp(\beta V_0) - 1][(1+\epsilon)^3 - 1] \simeq 3\epsilon \exp(\beta V_0), \tag{1.2}$$

where B_2^{SW} denotes the second virial coefficient of the SW potential (1.1), $B_2^{\mathrm{HS}} = 2\pi\sigma^3/3$ that of the HS of diameter σ, and $\beta = 1/k_B T$ is the inverse temperature. If we denote this constant value as

$$\frac{B_2^{\mathrm{HS}} - B_2^{\mathrm{AHS}}}{B_2^{\mathrm{HS}}} \equiv \frac{1}{4\tau} \tag{1.3}$$

so that the second virial coefficient of the AHS model reads, $B_2^{\mathrm{AHS}} = B_2^{\mathrm{HS}}(1 - 1/4\tau)$, then all the structural properties of the AHS system (see below) will depend only on the scaled distance r/σ, the dimensionless density or packing fraction $\eta = \pi\rho\sigma^3/6$ (ρ being the number density), and the adhesiveness parameter τ^{-1}. When $\tau \to \infty$ the AHS system reduces to the ordinary HS system, while for finite values of the adhesiveness parameter ($\tau^{-1} \neq 0$) the AHS system can be viewed as a system of HS with a strong ($V_0 \to \infty$) surface ($\epsilon \to 0$) adhesion (attraction). The total thermodynamic properties of the AHS system will, however, depend on η and on both τ and T. Within the AHS model the relation between τ and T is arbitrary. A specific relation between τ and T can be obtained [6] by returning to the condition, $B_2^{\mathrm{AHS}} = B_2^{\mathrm{SW}}$, underlying the limiting procedure defining the AHS model. We rewrite this relation as [see (1.2) and (1.3)]

$$\frac{T_0}{T} = \ln\left(1 + \frac{\tau_0}{\tau}\right), \tag{1.4}$$

where $T_0 = V_0/k_B$ and $\tau_0^{-1} = 4[(1+\epsilon)^3 - 1]$. For fixed values of T_0 and τ_0, Eq. (1.4) implies that $\tau \to \infty$ when $T \to \infty$ and $\tau \to 0$ when $T \to 0$, whereas for weak adhesiveness ($\tau_0 \ll \tau$) τ and T are proportional ($\tau \simeq \tau_0 T/T_0$). A relation such as (1.4) is useful if one wants to consider the AHS model as providing an approximate description of a system with a SW potential of the type given in (1.1). In this sense the AHS model has been used successfully for the interpretation of experiments on colloidal suspensions exhibiting strong short-ranged attractions of unknown form [7]. Phenomena such as aggregation, percolation and phase transitions can be studied in this way with the AHS model often providing closed-form expressions that can be directly fitted to the experimental data.

In the present study we will focus our attention on the phase behavior of the AHS system. The system exhibits a liquid-gas and a liquid-solid transition, and because of the strong attractions, also a sol-gel or percolation transition but the thermodynamic status of the latter is still unclear. While the PY predictions for the liquid-gas transition, and, to a lesser extent, also for the percolation transition, are in good agreement with the computer simulations [8], no such simulations exist as yet for the liquid-solid transition. The latter transition has been studied by Smithline and Haymet [9] within a perturbative density-functional theory and by Cerjan and Bagchi [10] from a bifurcation analysis. Here we will study the liquid-solid transition of AHS within the generalized effective liquid approach (GELA), a nonperturbative density-functional theory that gives an accurate picture of the liquid-solid transition of hard spheres [2], hard disks [11], and hard-sphere mixtures [12]. In the following section we first recall some of the structural and thermodynamic properties of the fluid phases of AHS within the PY approximation, including an explicit expression for its free energy. This information is used in Sec. III to study the solid phase of AHS within the GELA and to construct, in Sec. IV, the liquid-solid coexistence. Our conclusions are summarized in Sec. V.

II. THE FLUID PHASES OF AHS

As shown by Baxter [5], the PY approximation for the direct correlation function $c(r)$ of the fluid (both liquid and gas) phases of AHS can be written as

$$c(x;\eta,\lambda) = A_0(\eta,\lambda) + xA_1(\eta,\lambda) + \frac{1}{2}x^3\eta A_0(\eta,\lambda) - \frac{1}{12x}\eta\lambda^2 + \frac{1}{12}\lambda\delta(x-1) \tag{2.1}$$

for $0 \le x \le 1$ and $c(x;\eta,\lambda) = 0$ for $x > 1$. In (2.1), $x = r/\sigma$ is the interparticle distance r scaled with the HS diameter σ, $\eta = \pi\rho\sigma^3/6$ with ρ the number density, and λ is a dimensionless parameter given by

$$\lambda = \frac{6}{\eta}\left[\nu - (\nu^2-\gamma)^{1/2}\right], \tag{2.2a}$$

$$\nu = \tau + \frac{\eta}{1-\eta} \qquad \gamma = \frac{\eta(2+\eta)}{6(1-\eta)^2}, \tag{2.2b}$$

where τ is the adhesiveness parameter of (1.3), and

$$A_0(\eta,\lambda) = -\frac{[1+2\eta+\lambda\eta(\eta-1)]^2}{(1-\eta)^4}, \tag{2.3a}$$

$$A_1(\eta,\lambda) = \frac{\eta}{2(1-\eta)^4}[3(\eta+2)^2 + 2\lambda(\eta^3+6\eta^2-6\eta-1) + \lambda^2\eta(\eta^3-3\eta+2)]. \tag{2.3b}$$

From (2.1) one obtains, via the compressibility equation [4], the equation of state

$$Z(\eta,\tau) = \frac{1+\eta+\eta^2}{(1-\eta)^3} - \frac{\omega(2+\eta)}{2(1-\eta)^3} + \frac{\omega^3}{36\eta(1-\eta)^3}, \tag{2.4}$$

where $\omega = \lambda\eta(1-\eta)$ and $Z = \beta P/\rho$ is the compressibility factor, P being the pressure. The central quantity of interest here, f, the Helmhlotz free energy per particle of the fluid phases, can be obtained from

$$\beta f(\eta,\tau) = \ln\left(\frac{6\eta}{\pi}\right) + \psi(\eta,\tau) + 3\ln\left(\frac{\Lambda}{\sigma}\right) - 1, \tag{2.5}$$

where $\Lambda = h(2\pi m k_B T)^{-1/2}$ is the thermal de Broglie wavelength and ψ the reduced excess free energy per particle,

$$\psi(\eta,\tau) = \int_0^\eta d\eta' \, \frac{Z(\eta',\tau)-1}{\eta'}. \tag{2.6}$$

Substituting (2.4) in (2.6) one obtains (using a computer algebra method) the following explicit expression for $\psi(\eta,\tau)$:

$$\psi(\eta,\tau) = \psi_{\rm PY}(\eta) + 12\tau(6\tau-1)\ln B(\eta,\tau) - \sqrt{2}(54\tau^2-12\tau+1)\ln C(\eta,\tau) - 24\tau^3\frac{1-\eta}{\eta} + 36\tau^2 + 6\tau\frac{10\eta-1}{1-\eta} + \frac{3\eta(5\eta-4)}{(1-\eta)^2} + 2\tau\left[12\tau^2\frac{1-\eta}{\eta} - 30\tau - \frac{8\eta-5}{1-\eta}\right]A(\eta,\tau), \tag{2.7}$$

where $\psi_{\rm PY}(\eta)$ is the PY-HS result

$$\psi_{\rm PY}(\eta) = -\ln(1-\eta) + \frac{3\eta(2-\eta)}{2(1-\eta)^2} \tag{2.8}$$

and

$$A(\eta,\tau) = \left[1 + \frac{2\eta}{\tau(1-\eta)} + \frac{\eta(5\eta-2)}{6\tau^2(1-\eta)^2}\right]^{1/2}, \tag{2.9a}$$

$$B(\eta,\tau) = \frac{1}{2}[1+A(\eta)] + \frac{(6\tau-1)\eta}{12\tau^2(1-\eta)}, \tag{2.9b}$$

$$C(\eta,\tau) = 1 + 3\frac{\eta+\sqrt{2}\tau(1-\eta)[A(\eta)-1]}{[3\sqrt{2}\tau(1+\sqrt{2})-1](1-\eta)}. \tag{2.9c}$$

From (2.4) and (2.5) one obtains, finally, the chemical potential μ from $\beta\mu = \beta f + Z$. The equation of state (2.4) describes a liquid-gas transition with a critical point located at $\eta_c = (3\sqrt{2}-4)/2 \simeq 0.121$, $\tau_c = (2-\sqrt{2})/6 \simeq 0.097$, which is close to the simulation result [8]. Other equations of state can be derived from the virial or energy equations [5] but they do not appear to be consistent with the simulation results and we will therefore consider henceforth only the compressibility equation of

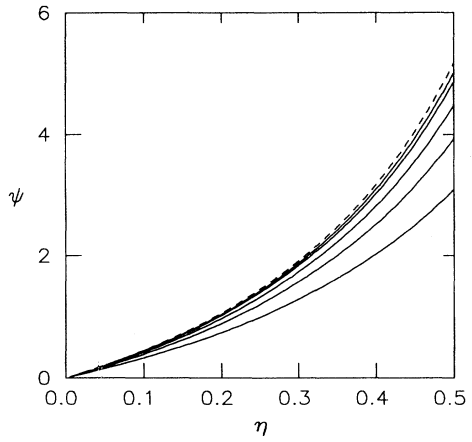

FIG. 1. Excess free energy per particle ψ [Eq. (2.7)] of the AHS fluid vs the packing fraction for (from bottom to top) $\tau = 1, 2, 4, 10, 20$ (solid lines). The dashed line corresponds to the ($\tau = \infty$) Percus-Yevick hard-sphere result.

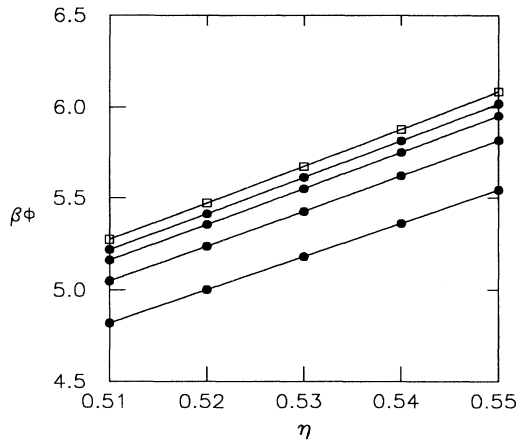

FIG. 2. Free energy per particle $\beta\phi = \beta f_s(\eta, \tau) - 3\ln(\Lambda/\sigma) + 1$ of the equilibrium AHS solid (solid dots) vs the packing fraction for (from bottom to top) $\tau = 5, 10, 20, 40$. The open squares correspond to the ($\tau = \infty$) Percus-Yevick hard-sphere result.

state (2.4). The way in which f of (2.5) approaches the HS limit is illustrated in Fig. 1.

III. THE AHS SOLID PHASE

If the periodic density of the solid $\rho(\mathbf{r})$ is parametrized in terms of Gaussians, i.e.,

$$\rho_s(\mathbf{r}) = \left(\frac{\alpha}{\pi}\right)^{3/2} \sum_j \exp[-\alpha(\mathbf{r} - \mathbf{r}_j)^2], \tag{3.1}$$

where the sum runs over the Bravais lattice vectors $\{\mathbf{r}_j\}$ of the crystal structure, then the Helmholtz free energy per particle of the solid (f_s) is obtained by minimizing $f_s(\eta, \tau; \alpha)$ with respect to the Gaussian width parameter α of (3.1), viz., $f_s(\eta, \tau) = \min_\alpha f_s(\eta, \tau; \alpha)$. Within the GELA, the variational free energy $f_s(\eta, \tau; \alpha)$ is given by [2]

$$\beta f_s(\eta, \tau; \alpha) = \frac{3}{2}\left[\ln\left(\frac{\alpha\sigma^2}{\pi}\right) - 1\right] + \psi(\eta_0(\alpha), \tau) + 3\ln\left(\frac{\Lambda}{\sigma}\right) - 1, \tag{3.2}$$

where ψ is still given by (2.7) and the ideal part of the free energy has already been replaced by its asymptotic large-α value of interest here [2]. The effective liquid density corresponding to (3.1), $\eta_0(\alpha)$, is determined (for each η and τ) from the self-consistency condition of the GELA [2],

$$\frac{\partial^2}{\partial\xi^2}[\xi\psi(\hat{\eta}(\alpha;\xi),\tau)] = -\sum_j \left(\frac{\alpha}{2\pi r_j^2}\right)^{1/2} \int_0^\infty dr\, r\, c(r/\sigma; \hat{\eta}(\alpha;\xi), \tau)\left[\exp\left(-\frac{\alpha}{2}(r - r_j)^2\right) - \exp\left(-\frac{\alpha}{2}(r + r_j)^2\right)\right], \tag{3.3}$$

where $0 \le \xi \le 1$ is a charging parameter and $c(x; \eta, \tau)$ is given by (2.1). From the solution of (3.3), satisfying the initial conditions $\hat{\eta}(\alpha; 0) = 0$ and $[\partial\hat{\eta}(\alpha, \xi)/\partial\xi]_{\xi=0} = 0$, one finally obtains the effective density, $\eta_0(\alpha) = \hat{\eta}(\alpha; 1)$, to be used in (3.2). Equation (3.3) can also be further transformed into an integral equation or into a system of two first-order differential equations. Here we have followed the latter procedure (see [11] for details).

For small values of the adhesiveness parameter ($\tau^{-1} \to 0$) the solutions of the AHS equations (3.2) and (3.3) approach smoothly the PY-GELA results [2] describing a stable face-centered-cubic (fcc) HS crystal (see Fig. 2). Increasing the adhesiveness from the HS limit ($\tau \to \infty$) to approximately $\tau \simeq 5$, the density for which the fcc crystal first stabilizes remains practically constant ($\eta \simeq 0.50$) but the spheres become slightly more delocalized [i.e., have a smaller α value (3.1)] when decreasing τ. For $\tau < 5$ the spheres continue to delocalize while the threshold density for finding a stable solid starts to increase reaching $\eta \simeq 0.55$ for $\tau = 1$. In between ($5 > \tau > 1$), the free energy of the solid turns from convex ($\tau = 5$) to concave ($\tau = 1$) with the transition occuring for $\tau \simeq 3$ (see Fig. 3). The rapid changes observed for $\tau < 5$ announce the incipient instability of the solid which becomes mechanically unstable (negative compressibility) for $\tau < 3$. When τ is interpreted as a measure of the temperature T [see (1.4)] this behavior is counterintuitive, since lowering the temperature should make it more easy for the solid to appear. On this and similar grounds (see also [9]) the behavior of the AHS model could be termed pathological. Although this cannot be ruled out completely, we would like to propose here a different interpretation for this behavior of the AHS. It is known [8] that increasing the adhesiveness

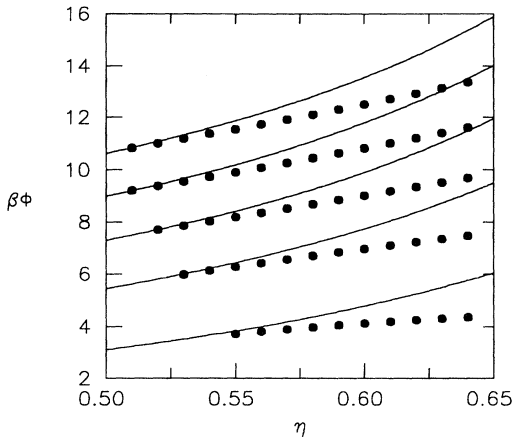

FIG. 3. Free energy per particle $\beta\phi = \beta f_s(\eta,\tau) - 3\ln(\Lambda/\sigma) + 1$ of the equilibrium AHS solid (solid dots) vs the packing fraction for (from bottom to top) $\tau = 1, 2, 3, 4, 5$. The solid lines correspond to the free energy per particle of the AHS fluid $\beta\phi = \ln(6\eta/\pi) + \psi(\eta,\tau)$ at the same τ values. To separate the curves the $\beta\phi$ scales have been shifted by $1.5 \times (\tau - 1)$, with the scale shown corresponding to $\tau = 1$. For $\tau < 3$ the free energy of the solid is seen to become concave (negative compressibility).

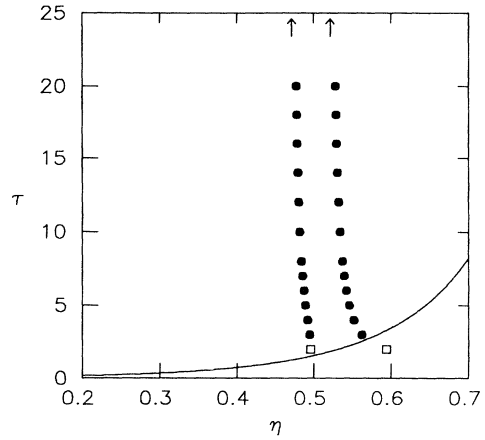

FIG. 4. The liquid-solid coexistence of AHS in the τ-η plane as obtained from the GELA (solid dots). The arrows indicate the HS ($\tau = \infty$) results. The open squares correspond to the liquid-solid coexistence for $\tau = 2$ where the solid is mechanically unstable (see Fig. 3). The solid line indicates the PY percolation transition [Eq. (4.2)].

(decreasing τ) also greatly increases the probability for the formation of an aggregating cluster in the AHS system. It is therefore remarkable that the solid becomes mechanically unstable precisely in the region where the PY theory predicts the occurrence of a percolating cluster (see Fig. 4). It is thus plausible that there exists in the AHS system a competition between the stabilizing effect on the solid of lowering the temperature and the destabilizing effect due to increased aggregation with the latter winning for $\tau < 3$. In other words, there appears to be a competition between the liquid-solid and the percolation transitions leading, for $\tau < 3$, to the formation of a gel-like phase as the result of the strong attractions. Finally, in a third and less optimistic interpretation one could also ascribe the above behavior to an artifact of the theory, a possibility that cannot be excluded except by performing further computer simulations.

IV. THE LIQUID-SOLID COEXISTENCE

With the aid of the free energy f of the liquid phase [see (2.5)] and of the solid phase [see (3.2)] one can construct the liquid-solid phase diagram of the AHS. To this end we solve the two-phase coexistence conditions of equality of the pressures (P) and the chemical potentials (μ) of the two phases for various values of the temperature (T). The latter quantities are obtained from the free energy f by using the thermodynamic relations $P/\rho = \eta\partial f/\partial\eta$ and $\mu = \partial(\eta f)/\partial\eta$. As already indicated in Sec. I, the (total) free energy f depends on both T and τ. If we assume that the equality of T in both phases implies the equality of τ then the two-phase coexistence conditions can be reduced to equations involving only $\eta_{L(S)}$ and τ [where L(S) refers to the liquid (solid) phase]. This, however, is not the case for the Clausius-Clapeyron equation [4]

$$\left(\frac{\partial P}{\partial T}\right)_{\text{coex}} = \frac{s_L - s_S}{v_L - v_S}, \tag{4.1}$$

where s is the entropy per particle and $v = 1/\rho$, since the evaluation of the left-hand side of (4.1) requires an explicit knowledge of the relation between τ and T [such as the one given in (1.4)] (see also Fig. 5).

The results for the L-S coexistence of AHS, as obtained from the PY-GELA equations [(2.5),(3.2)], are given in Table I. The trends are as generally expected for a L-S transition: the width of the transition increases when

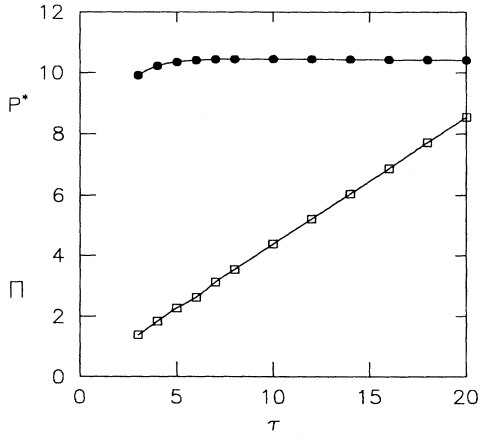

FIG. 5. The pressure vs τ at the liquid-solid coexistence of AHS for two different reductions. Solid dots: $P^* = \beta P\sigma^3$. Open squares: $\Pi = \Pi^*/25$ with $\Pi^* = P\sigma^3/k_BT_0 = TP^*/T_0$ where T/T_0 is obtained from Eq. (1.4) with $\tau_0 = 1$. Notice that Π^* provides a correct behavior for Eq. (4.1).

TABLE I. Solid-liquid coexistence data for AHS vs τ. Here η_F and η_S denote the coexisting packing fractions of the fluid and solid phases, and $P^* = \beta P\sigma^3$ and $\mu^* = \beta\mu$ are, respectively, the dimensionless pressure and chemical potential at coexistence. $\chi = \eta_S/\eta_F - 1$ denotes the fractional density change while $L = [3/(2\alpha d^2)]^{1/2}$ is the Lindemann ratio with α the Gaussian width parameter and d the nearest-neighbor distance of the fcc lattice.

τ	η_F	η_S	P^*	μ^*	χ	L
3	0.4947	0.5623	9.9130	14.6216	0.1365	0.117
4	0.4918	0.5519	10.2268	15.1443	0.1223	0.119
5	0.4891	0.5460	10.3566	15.4015	0.1162	0.119
6	0.4870	0.5420	10.4146	15.5448	0.1130	0.120
7	0.4852	0.5392	10.4411	15.6321	0.1112	0.120
8	0.4838	0.5370	10.4524	15.6888	0.1100	0.120
10	0.4817	0.5341	10.4550	15.7546	0.1088	0.120
12	0.4802	0.5321	10.4489	15.7903	0.1082	0.120
14	0.4790	0.5306	10.4404	15.8114	0.1077	0.120
16	0.4781	0.5295	10.4317	15.8248	0.1073	0.120
18	0.4774	0.5286	10.4237	15.8338	0.1071	0.120
20	0.4769	0.5279	10.4163	15.8401	0.1069	0.120
40	0.4742	0.5246	10.3735	15.8576	0.1064	0.120
∞	0.4713	0.5213	10.3118	15.8545	0.1062	0.120

lowering T (or τ) while the Lindemann ratio remains constant along the melting line. One exception concerns the fact that the densities (η_L and η_S) increase when lowering T (or τ). As argued in Sec. III and shown in Fig. 3, this is an indication of the incipient instability of the solid phase when approaching the (PY) percolation transition [13] given by

$$\tau = \frac{19\eta^2 - 2\eta + 1}{12(1-\eta)^2}. \tag{4.2}$$

In Table II we compare some of our predictions with those of the previous theoretical attempts [9,10]. We have found no trace of the reentrant liquid phase found in [9]. Needless to say, the respective merits of the different theoretical approximations can only be assessed by performing computer simulations of the L-S transition of AHS, a study which at present is still missing.

TABLE II. Comparison of the solid-liquid coexistence data for AHS as obtained from different theoretical approximations.

τ	$\rho_F\sigma^3$	$\rho_S\sigma^3$	P^*
3	1.027[a]	1.103[a]	14.2678[b]
	0.945[c]	1.074[c]	9.9130[c]
5	1.008[a]	1.079[a]	14.4858[b]
	0.934[c]	1.043[c]	10.3566[c]
	0.885[d]	1.110[d]	8.3274[b]
10	0.988[a]	1.058[a]	14.3325[b]
	0.920[c]	1.020[c]	10.4550[c]
∞	0.966[a]	1.034[a]	14.0985[b]
	0.900[e]	0.996[e]	10.3118[e]
	0.884[d]	1.085[d]	9.5665[b]

[a]From Smithline and Haymet (Ref. [9]).
[b]From Eq. (2.4).
[c]From this work.
[d]From Cerjan and Bagchi (Ref. [10]).
[e]From Tejero and Cuesta (Ref. [11]).

V. CONCLUSIONS

A sytem of adhesive hard spheres can be viewed as a rough approximation for certain colloidal supensions with strong attractions [7]. The direct correlation function of the fluid phases (both liquid and gas) of AHS within the Percus-Yevick approximation has been given in closed form by Baxter [5]. Here we have obtained the corresponding closed-form expression (2.7) for the free energy of these fluid phases. These expressions have been used then as input information in a nonperturbative density-functional study of the solid phase and the liquid-solid transition of AHS. Within the generalized effective liquid approximation (GELA) the liquid-solid transition of AHS is found to exhibit most of the freezing features of simple liquids. In the region where the liquid-solid transition of the GELA crosses the (PY) percolation transition (which would correspond to a gel formation for the colloidal suspensions), the solid is shown to become mechanically unstable. This precludes the existence (within the GELA) of a direct connection between the liquid-solid and the liquid-gas transitions, and hence the existence of a gas-liquid-solid triple point. Further computer simulations are necessary in order to assess the validity of this scenario.

ACKNOWLEDGMENTS

C. F. Tejero wishes to acknowledge the support of the Dirección General de Investigación Científica y Técnica (DGICYT, Spain) (PB91-0378). M. Baus acknowledges the financial support of the Fonds National de La Recherche Scientifique and also of the Association Euratom-Etat Belge.

[1] For recent reviews, see, e.g., Y. Singh, Phys. Rep. **207**, 351 (1991); M. Baus, J. Phys. Condens. Matter **2**, 2111 (1990); A. D. J. Haymet, Ann. Rev. Phys. Chem. **38**, 89 (1987).
[2] A. Kyrlidis and R. A. Brown, Phys. Rev. A **45**, 5654 (1992); J. F. Lutsko and M. Baus, *ibid.* **41**, 6647 (1990), and references therein.
[3] A. Kyrlidis and R. A. Brown, Phys. Rev. E **47**, 427 (1993); C. F. Tejero, J. F. Lutsko, J. L. Colot, and M. Baus, Phys. Rev. A **46**, 3373 (1992), and references therein.
[4] J. P. Hansen and I. R. McDonald, *Theory of Simple Liquids* (Academic, London, 1986).
[5] R. J. Baxter, J. Chem. Phys. **49**, 2270 (1968); Aust. J. Phys. **21**, 563 (1968); in *Physical Chemistry—An Advanced Treatise*, edited by D. Henderson (Academic, New York, 1971), Vol. 8A; R. O. Watts, D. Henderson, and R. J. Baxter, Adv. Chem. Phys. **21**, 421 (1971).
[6] B. Barboy, J. Chem. Phys. **61**, 3194 (1974).
[7] M. C. Grant and W. B. Russel, Phys. Rev. E **47**, 2606 (1993), and references therein.
[8] N. A. Seaton and E. D. Glandt, J. Chem. Phys. **87**, 1785 (1987); W. G. T. Kranendonk and D. Frenkel, Mol. Phys. **64**, 403 (1988).
[9] S. J. Smithline and A. D. J. Haymet, J. Chem. Phys **83**, 4103 (1985).
[10] C. Cerjan and B. Bagchi, Phys. Rev. A **31**, 1647 (1985).
[11] C. F. Tejero and J. A. Cuesta, Phys. Rev. E **47**, 490 (1993).
[12] H. Xu and M. Baus, J. Phys. Condens. Matter **4**, L663 (1992).
[13] Y. C. Chiew and E. D. Glandt, J. Phys. A **16**, 2599 (1983).